Science Advances

AAAS

advances.sciencemag.org/cgi/content/full/4/5/eaar6179/DC1

Supplementary Materials for

Substrate-modulated unwinding of transmembrane helices in the NSS transporter LeuT

Patrick S. Merkle, Kamil Gotfryd, Michel A. Cuendet, Katrine Z. Leth-Espensen, Ulrik Gether, Claus J. Loland, Kasper D. Rand

Published 11 May 2018, *Sci. Adv.* **4**, eaar6179 (2018)
DOI: 10.1126/sciadv.aar6179

This PDF file includes:

SUPPLEMENTARY MATERIALS

Supplementary Materials and Methods

Purification of LeuT

Briefly, detergent-solubilized LeuT was immobilized on Chelating Sepharose Fast Flow resin (GE Healthcare), extensively washed with ice-cold Buffer A containing step imidazole gradient (60-100 mM), and eluted in the same buffer supplemented with 300 mM imidazole. Sample purity was evaluated by SDS-PAGE analysis and protein concentration was determined by measuring the UV_{280} absorbance (ε = 1.91 cm^2/ml). LeuT fractions with the highest protein concentrations were pooled and dialyzed against imidazole-free Buffer A for at least 16 h using 0.5 ml Slide-A-Lyzer MINI dialysis devices (10 kDa MWCO; Thermo Fisher Scientific). Dialyzed LeuT samples were stored as small aliquots at -80 °C until further use.

Purification of MSP1D1

MSP1D1 was isolated by nickel affinity chromatography and sample purity evaluated by SDS-PAGE analysis. The polyhistidine tag was removed by overnight incubation of purified MSP1D1 in the presence of 3% (w/w) tobacco etch virus protease under constant rotation at room temperature. Cleaved MSP1D1 protein was collected using nickel affinity chromatography and dialyzed against buffer containing 20 mM Tris-HCl, pH 8.0, and 100 mM NaCl. Following up-concentration of MSP1D1 to 4 mg/ml using spin filter units (Vivaspin centrifugal concentrator, 10 kDa MWCO, Sartorius Biotech), sample aliquots were stored at -80 °C until further use.

Scintillation Proximity Assay

Briefly, for saturation binding, 0.5 µg/ml of purified LeuT was mixed with 0.125 mg/ml YSi-Cu His-Tag SPA beads (PerkinElmer) and varying concentrations of [^{3}H]leucine (PerkinElmer, 10.8 Ci/mmol), all diluted in binding buffer (20 mM Tris-HCl, pH 8.0, 200 mM NaCl, 0.05% (w/v) DDM). Na^+-dependency was determined using fixed 100 nM [^{3}H]leucine, in assay buffer supplemented with varying concentrations of NaCl while ionic strength was maintained with KCl. Nonspecific background was determined in the presence of unlabeled leucine. Binding of [^{3}H]leucine was monitored employing MicroBeta scintillation counter (PerkinElmer) and data were fitted using the GraphPad Prism 6 software to a one-site saturation or dose-response function to obtain K_d and EC_{50} values, respectively.

Hydrogen/Deuterium Exchange of Detergent-Solubilized LeuT

To obtain the Na^+ and Cs^+ states, purified LeuT was dialyzed overnight using 0.5 ml Slide-A-Lyzer MINI dialysis devices (10 kDa MWCO) at 4 °C against modified Buffer A containing 20 mM Tris-HCl, pH 8.0, 0.05% (w/v) DDM, 20% (v/v) glycerol, and either 200 mM NaCl or 200 mM CsCl. The K^+_{High} state was obtained by manually adding a stock solution containing 20 mM Tris-HCl, pH 8.0, 0.05% (w/v) DDM, and 3.2 M KCl to the purified LeuT stock to reach a final KCl concentration of 800 mM. Two different Leu states were prepared and analyzed in the present study. First, we studied the HDX of LeuT in presence of 200 mM NaCl and a non-saturating leucine concentration. For this reason, NaCl was manually added to the purified LeuT stock to a final concentration of 200 mM, whereas leucine was present in the deuterated buffer. The leucine concentration during the labeling reaction was 1 µM, which resulted in approximately 60% transporter occupancy. Note that LeuT was not equilibrated with the substrate leucine prior to the labeling reaction. Second, we prepared samples, in which LeuT was equilibrated with a 3-fold molar excess of leucine prior to deuteration. Thereby, NaCl and leucine were manually added to the purified LeuT stock to a final concentration of 200 mM and 50 µM, respectively, which resulted in >99% transporter occupancy.

Reconstitution of LeuT into Phospholipid-Containing Bilayer Nanodiscs

Preparation of phospholipids and nanodisc assembly were performed in a similar manner as described previously. The phospholipids 1-palmitoyl-2-oleoyphosphatidylcholine (POPC) (Avanti Polar Lipids) and 1-

palmitoyl-2-oleyl-sn-glycero-3-phosphoracglycerol (POPG) (Avanti Polar Lipids) were prepared in chloroform and mixed in a 3:2 molar ratio. Chloroform was evaporated under nitrogen gas for 1 h and residual solvent removed by overnight incubation under vacuum. The thin lipid film was resuspended in buffer containing 10 mM Tris-HCl, pH 7.5, 100 mM choline chloride (ChCl), and 80 mM sodium cholate to a final lipid concentration of 50 mM.

LeuT, MSP, lipids, and DDM detergent were mixed in a molar ratio of 0.1:1:80:240, respectively, and incubated on ice for 1 h. Detergent was removed by addition of 80% (w/v) Biobeads (Bio-Rad SM-2 Resin) and left for 1 h on ice prior to overnight incubation at 4 °C. Loaded nanodiscs were separated from empty nanodiscs by nickel affinity chromatography and eluted in buffer containing 20 mM Tris-HCl, pH 8.0, 200 mM KCl, and 300 mM imidazole. Loaded nanodiscs were subsequently subjected to size-exclusion chromatography using a Superdex 200 10/300 GL column (GE Healthcare) pre-equilibrated with 20 mM Tris-HCl, pH 7.50, and 100 mM ChCl.

Hydrogen/Deuterium Exchange of LeuT Reconstituted into Nanodiscs

Samples of LeuT reconstituted into nanodiscs were buffer exchanged into buffer containing 20 mM Tris-HCl, pH 8.0, and 200 mM KCl. HDX was initiated by diluting LeuT 10-fold in a matching deuterated buffer and the samples labeled at 25 °C for various time intervals (i.e., 0.25-60 min). A total of 43 µl of ice-cold quench solution (0.5% formic acid and 6 M urea) was added to 50 µl of sample solution at the indicated time-points to lower pH to 2.5 and thus inhibit the isotopic exchange reaction. The quenched protein samples were kept on ice for the following sample preparation to minimize back-exchange. The nanodiscs were disassembled by adding an ice-cold stock solution of sodium cholate to reach a sodium cholate:lipid ratio of 25:1, respectively. Subsequently, approximately 1 µg LeuT was subjected to offline proteolysis at pH 2.5 for 2 min on ice by adding 6 µg porcine pepsin. In the last minute of proteolysis, the quenched sample was transferred into a cooled spin filter (Costar Spin-X® 2 mL centrifuge tube filter 0.45 µm cellulose acetate) containing 3 mg zirconia-coated silica particles (HybridSPE®-Phospholipid cartridge, Supelco). The quenched sample was centrifuged at 0 °C and 3000 g for 1 min and the flow through collected. Finally, quenched protein samples were immediately frozen and stored at -80 °C until further use.

Liquid Chromatography

Peptic peptides were trapped on a C18 column (ACQUITY UPLC BEH C18 1.7 µm VanGuard column Waters, Milford, USA) and the sample efficiently desalted for 3 min with mobile phase A (0.23% (v/v) formic acid, pH 2.5) at a constant flow rate of 200 µl/min. Peptides were gradually eluted by applying a 9 min linear gradient at a 40 µl/min flow rate and increasing concentrations (8% - 50% (v/v)) of mobile phase B (acetonitrile, 0.23% (v/v) formic acid). Chromatographic separation was accomplished by using a C18 guard column (ACQUITY UPLC BEH C18 1.7 µm VanGuard column Waters, Milford, USA) and a C18 analytical column (ACQUITY UPLC BEH C18 1.7 µm, 1x100 mm column Waters, Milford, USA).

Mass Spectrometry

All HDX-MS data was obtained using the sample preparation workflows described above and in the main body of the manuscript, however data presented in Fig. 5A was obtained employing a more sensitive Synapt G2-Si mass spectrometer as opposed to the Synapt G2 mass spectrometer used in all other experiments. Thus, while the two datasets shown in Fig. 5A and 5B can be compared qualitatively (i.e., in terms of comparing regions of the LeuT backbone, in which Cs^+ and K^+ induces changes in HDX), the relative magnitudes in ΔHDX might differ due to differences in the MS setup and thus a direct comparison of ΔHDX values between Fig. 5A and 5B should be avoided.

HDX Data Analysis

To determine the number of backbone amide hydrogens undergoing correlated exchange (#NHs), we first calculated the difference in HDX between the low- and high-mass population (ΔHDX, n=3) and corrected this value according to the measured back-exchange (BE, defined in Materials and Methods) of the respective peptide by using the following equation

$$\#\mathrm{NHs} = \left(\frac{\Delta\mathrm{HDX} \times 100\%}{100\% - \mathrm{BE}}\right)$$

To approximate critical kinetic measures (i.e., k_{op} and the half-life of the folded state) for individual unfolding events in LeuT, we first determined the relative abundance of the two isotopic envelopes for a given peptide using HX-Express 2.0. We subsequently plotted the relative abundance of the low-mass population (n=3) against labeling time (i.e., 0.25-60 min) based on HDX data for LeuT in K^+ reference state. Finally, the GraphPad Prism 6 software was used to fit the individual data-points to the following exponential decay function

$$y = \exp^{-k_{op} \times x}$$

in order to obtain the best-fit values for the kinetic parameters. HDX results were mapped onto the LeuT crystal structure (pdb 2A65) using Pymol (http://pymol.sourceforge.net/).

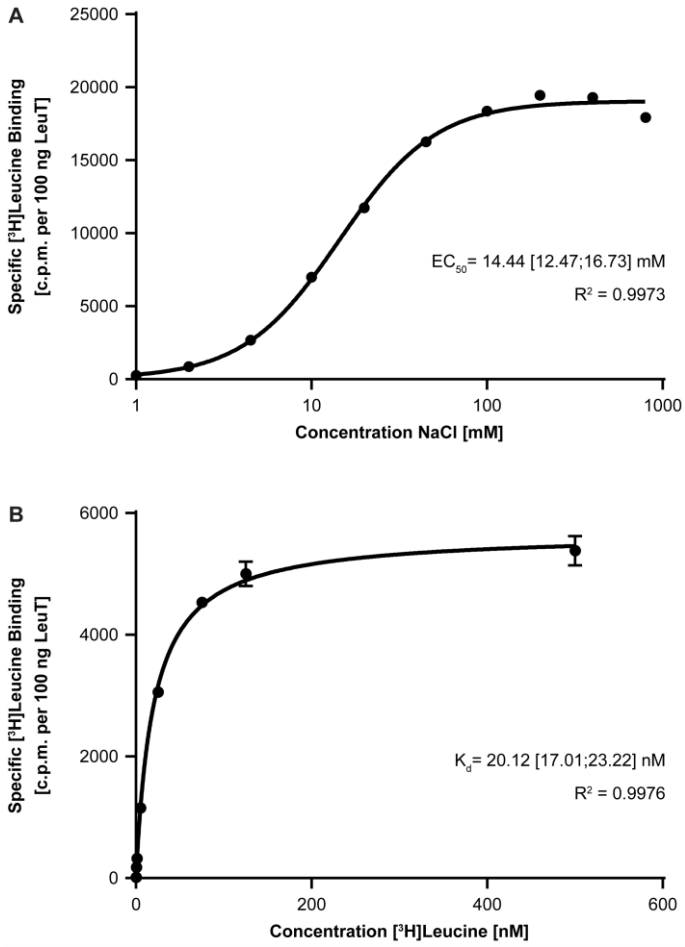

fig. S1. Na^+-dependent binding of [^{3}H]leucine to purified LeuT. The activity of purified LeuT was evaluated by assessing its binding affinity for [^{3}H]leucine and Na^+-dependency by SPA. (**A**) Dose-response curve for purified LeuT in the presence of fixed 100 nM [^{3}H]leucine and varying concentrations of NaCl. The calculated EC_{50} value for Na^+ was 14 [12;17] mM (mean [95% confidence interval], n=3). (**B**) One-site saturation curve for purified LeuT in the presence of 200 mM NaCl and varying concentrations of [^{3}H]leucine. The calculated K_d for [^{3}H]leucine was 20 [17;23] nM (n=2).

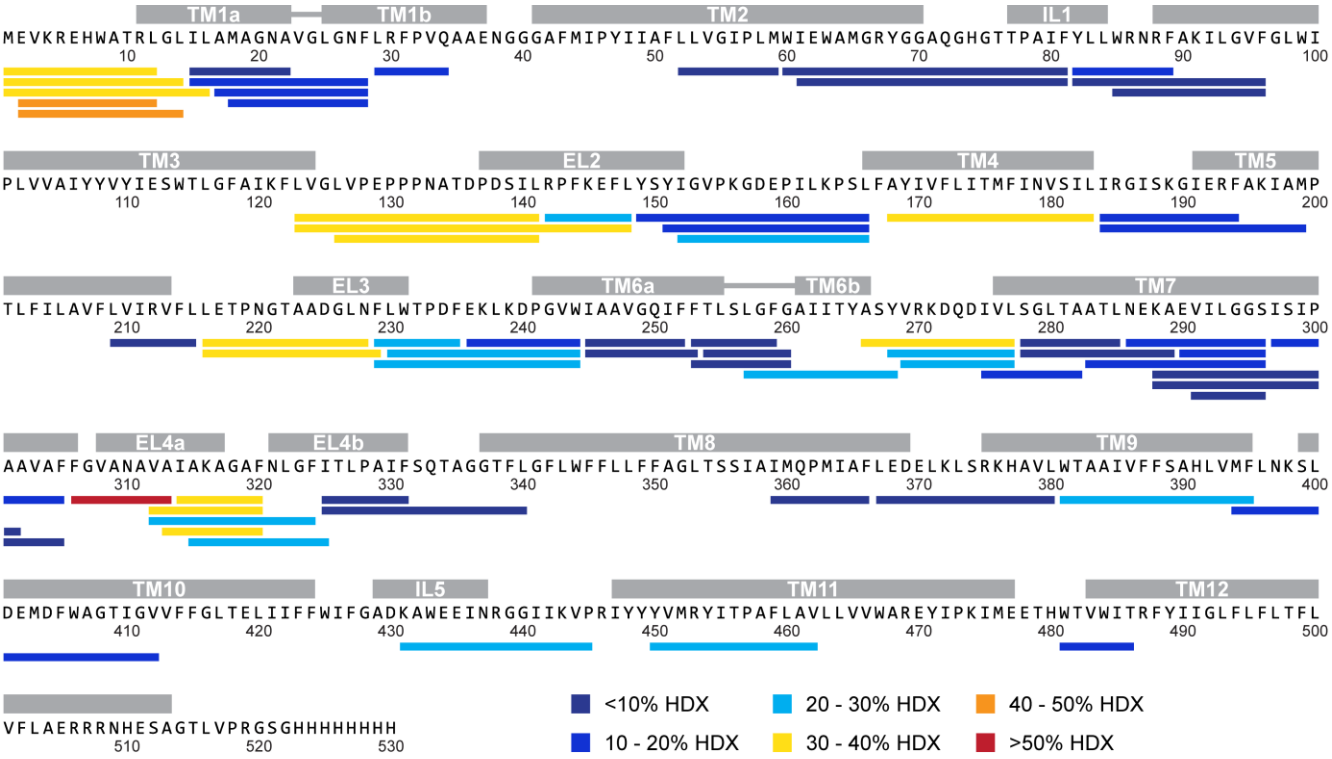

fig. S2. Correlation between the measured HDX and secondary structure elements in LeuT. The sequence coverage map for LeuT is shown. Individual structural motifs in LeuT are indicated above the protein sequence in grey color. Identified peptides are depicted as colored bars and are aligned with the corresponding LeuT sequence. Individual peptides are colored according to the measured deuteration level at the earliest measured time-point (0.25 min) for the K^+ reference state (cf. color scheme). Deuteration levels were obtained by comparing for each peptide the measured relative deuterium uptake with a theoretical, maximal deuterium uptake value (maximal deuterium uptake = number of residues – N-terminus – number of proline residues). Only the low-mass population was considered for peptides displaying bimodal isotopic envelopes. Notably, the more flexible loop regions appeared to exchange faster than individual TM helices.

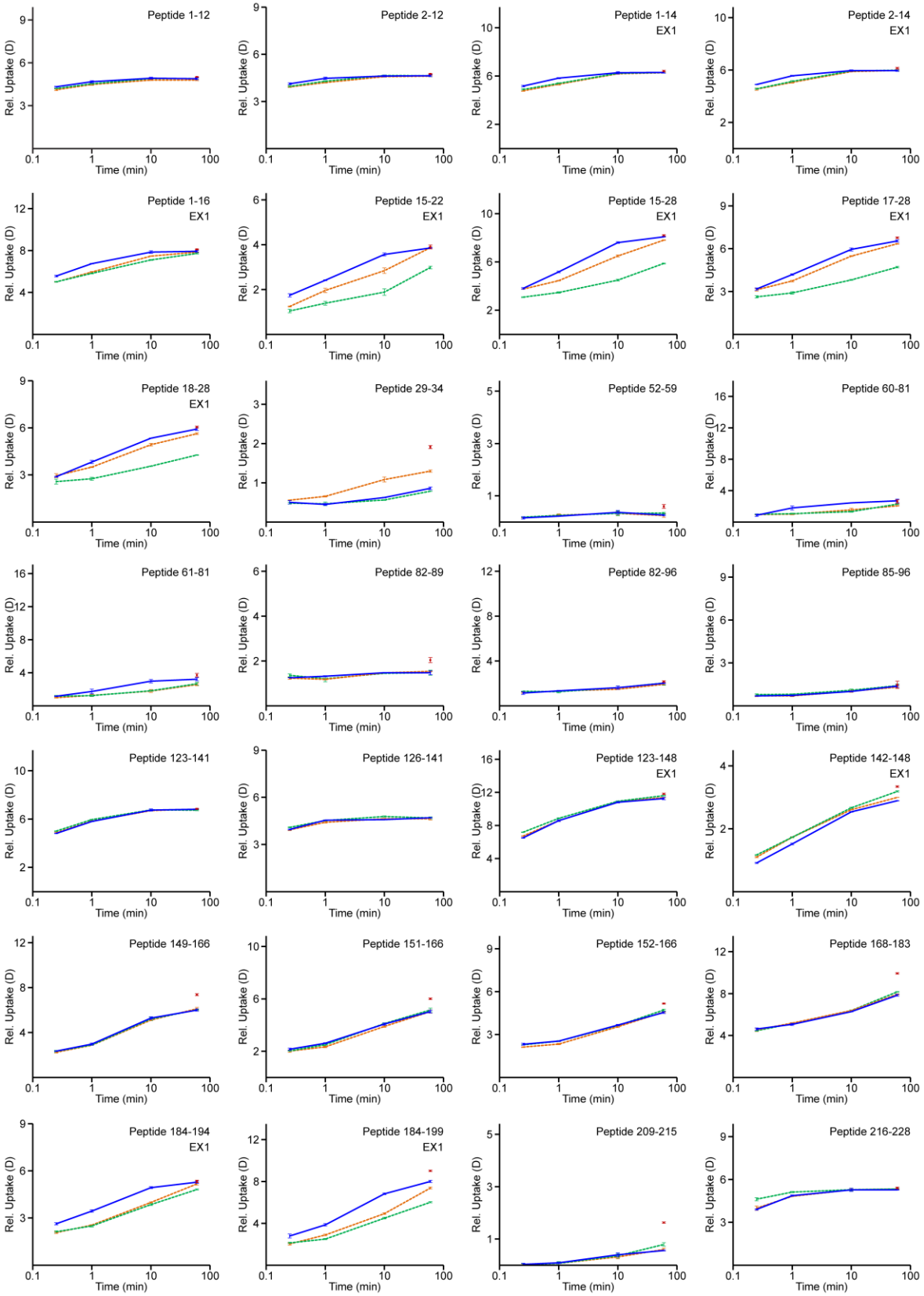
Peptide 1-12
Peptide 2-12
Peptide 1-14 EX1
Peptide 2-14 EX1
Peptide 1-16 EX1
Peptide 15-22 EX1
Peptide 15-28 EX1
Peptide 17-28 EX1
Peptide 18-28 EX1
Peptide 29-34
Peptide 52-59
Peptide 60-81
Peptide 61-81
Peptide 82-89
Peptide 82-96
Peptide 85-96
Peptide 123-141
Peptide 126-141
Peptide 123-148 EX1
Peptide 142-148 EX1
Peptide 149-166
Peptide 151-166
Peptide 152-166
Peptide 168-183
Peptide 184-194 EX1
Peptide 184-199 EX1
Peptide 209-215
Peptide 216-228
Rel. Uptake (D)
Time (min)

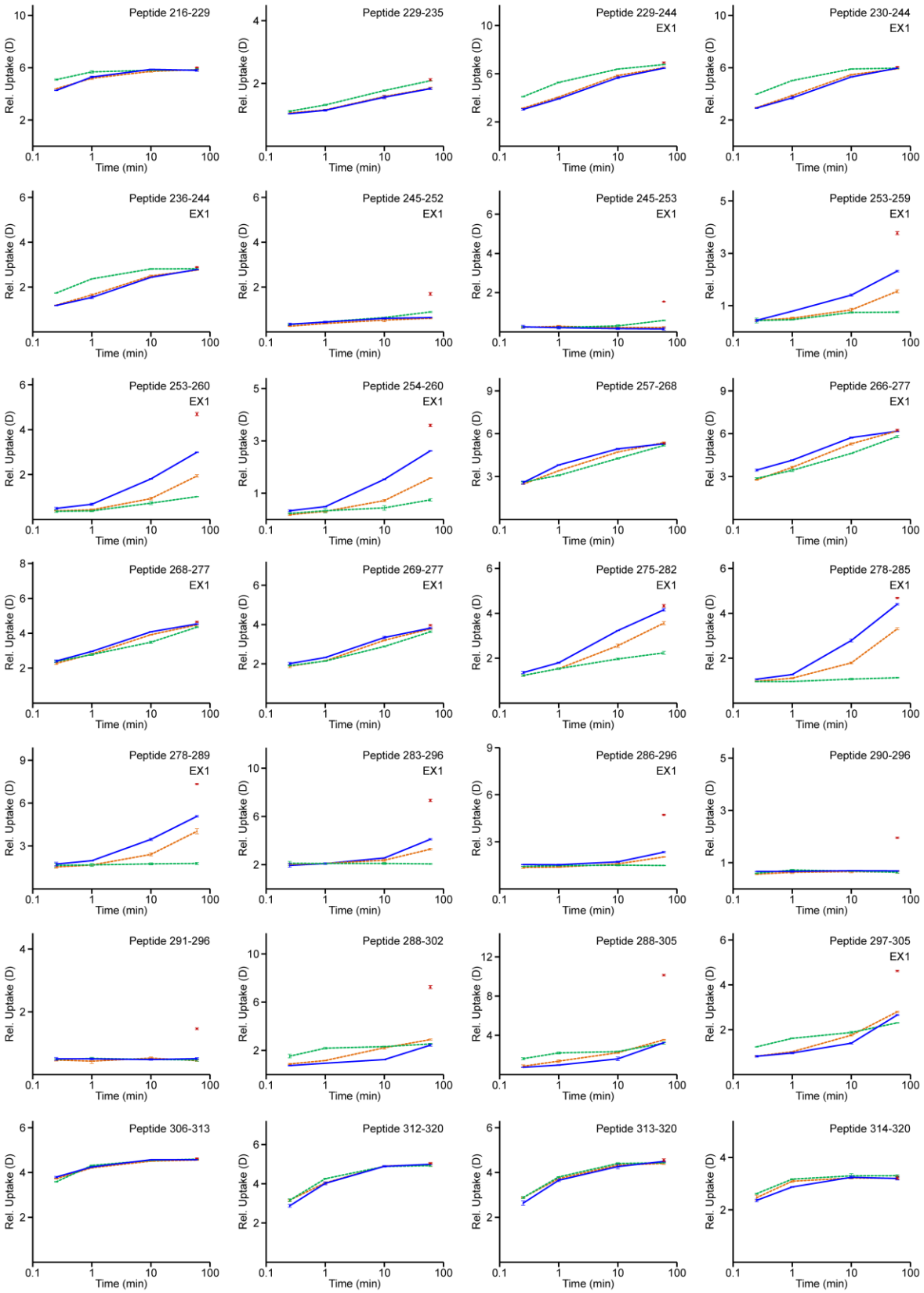
Peptide 216-229
Peptide 229-235
Peptide 229-244 EX1
Peptide 230-244 EX1
Peptide 236-244 EX1
Peptide 245-252 EX1
Peptide 245-253 EX1
Peptide 253-259 EX1
Peptide 253-260 EX1
Peptide 254-260 EX1
Peptide 257-268
Peptide 266-277 EX1
Peptide 268-277 EX1
Peptide 269-277 EX1
Peptide 275-282 EX1
Peptide 278-285 EX1
Peptide 278-289 EX1
Peptide 283-296 EX1
Peptide 286-296 EX1
Peptide 290-296
Peptide 291-296
Peptide 288-302
Peptide 288-305
Peptide 297-305 EX1
Peptide 306-313
Peptide 312-320
Peptide 313-320
Peptide 314-320
Rel. Uptake (D)
Time (min)

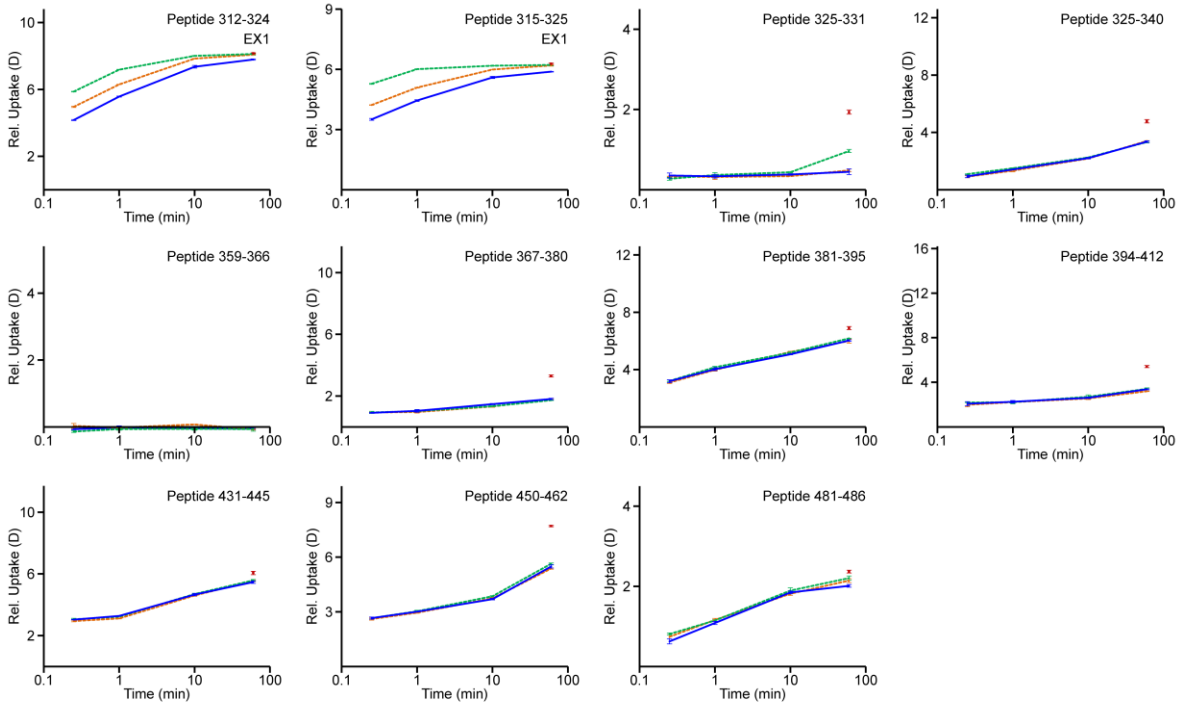

fig. S3. Deuterium uptake plots for detergent-solubilized LeuT. Deuterium uptake plots for all identified LeuT peptides are presented. The measured relative deuterium uptake for individual LeuT peptides is plotted against labeling time (i.e., 0.25-60 min). Blue, orange, and green curves illustrate the relative deuterium uptake for detergent-solubilized LeuT in the K^+, Na^+, and Leu state, respectively. The red colored square at the 60 min time-point indicates the measured relative deuterium uptake for the equilibrium-labeled control sample. Values represent means of three independent measurements. The corresponding standard deviations are indicated but are in most instances too small to be visible. For peptides displaying EX1 kinetics or signs thereof upon deuteration (marked as 'EX1'), we plotted an intensity-weighted, average deuterium uptake value accounting for both the low- and high-mass population. The HDX-MS data presented in this figure is also partially shown in form of difference charts in Fig. 2A and 2B.

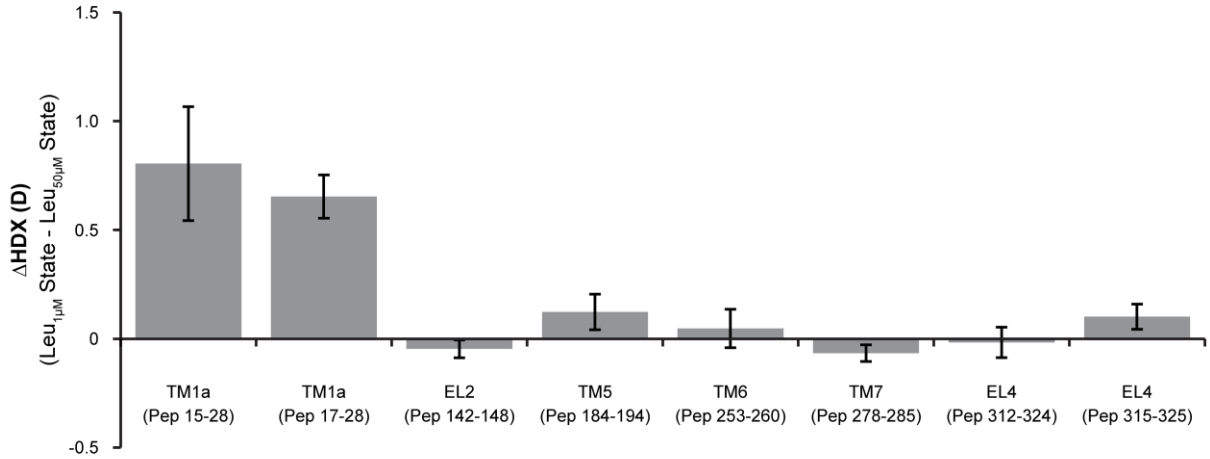

fig. S4. Impact of different leucine concentrations on local HDX rates in LeuT. The average relative deuterium uptake of the $Leu_{50\mu M}$ state is subtracted from the average value of the $Leu_{1\mu M}$ state for each peptide that is shown (cf. Supplementary Materials and Methods). These LeuT peptides were identified to be the most sensitive ones to Na^+ and leucine binding (cf. Fig. 2A and 2B) and they are denoted along the x-axis. Differences in HDX (ΔHDX) between the two leucine-bound states are plotted on the y-axis. Positive and negative ΔHDX values indicate increased and decreased HDX in the $Leu_{1\mu M}$ state, respectively. Values represent means and standard deviations of three independent measurements for the 0.25 min time-point. Notably, increasing the molar ratio between leucine and LeuT resulted in decreased HDX in TM 1a but did not impact the exchange rate of other structural motifs of the transporter.

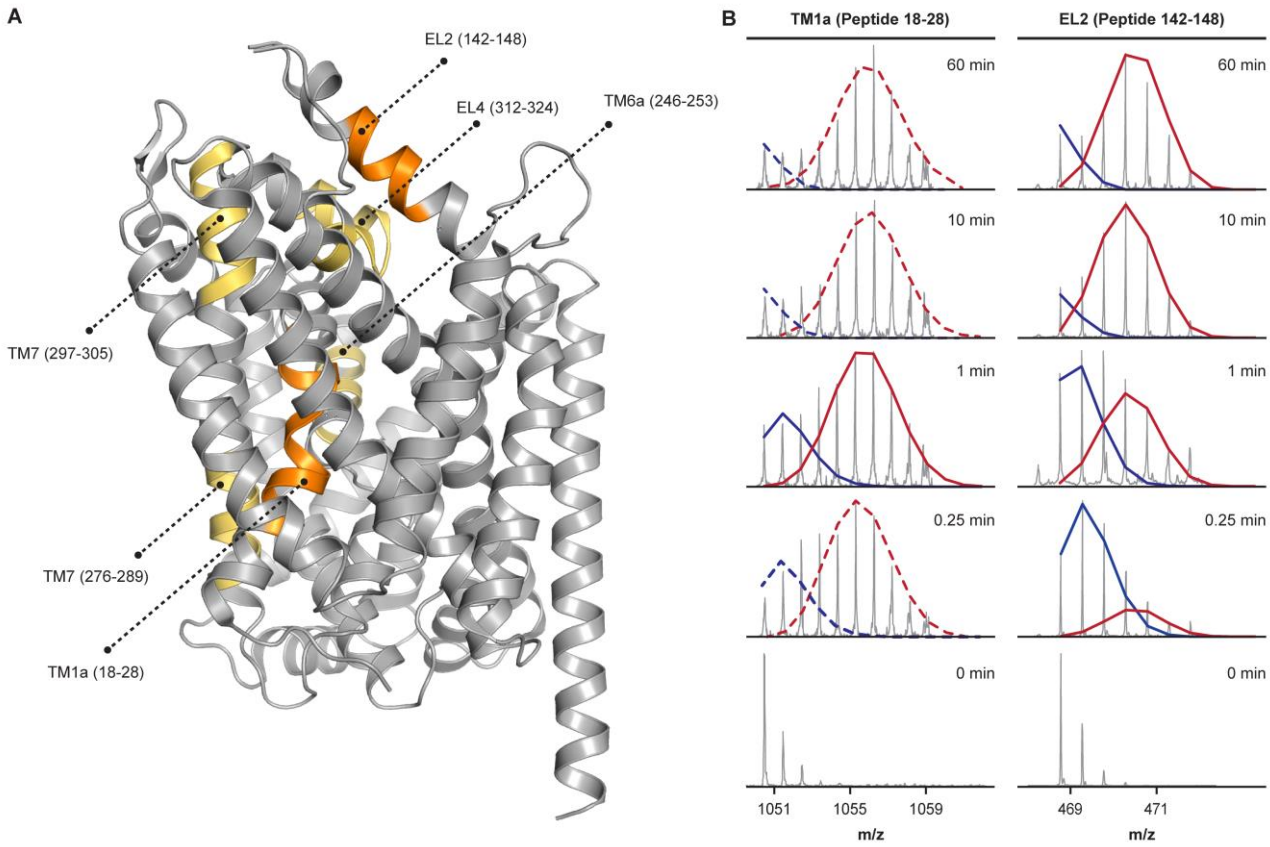

fig. S5. Partial unwinding of individual helices in LeuT reconstituted into phospholipid-containing bilayer nanodiscs. (**A**) LeuT segments that exchanged *via* an EX1 regime when the transporter was labeled in a phospholipidic environment are colored in orange in the LeuT crystal structure (pdb 2A65). LeuT segments for which we observed signs of EX1 kinetics but for which bimodal deconvolution could not be performed are indicated in yellow. (**B**) Representative mass spectra for individual peptides covering TM 1a and EL2 are shown for LeuT reconstituted into nanodiscs and in the presence of 200 mM K^+. The bimodal isotopic envelopes can be fitted to a low- (blue) and high-mass (red) population. Bimodal deconvolution was accomplished using HX Express 2.0 (solid lines). In some instances, bimodal deconvolution did not result in a qualitatively meaningful fit and the depicted low- and high-mass population (dashed lines) was adjusted manually for visual guidance. Notably, we observe a time-dependent interconversion of the low- and high-mass population compatible to an EX1 exchange regime.

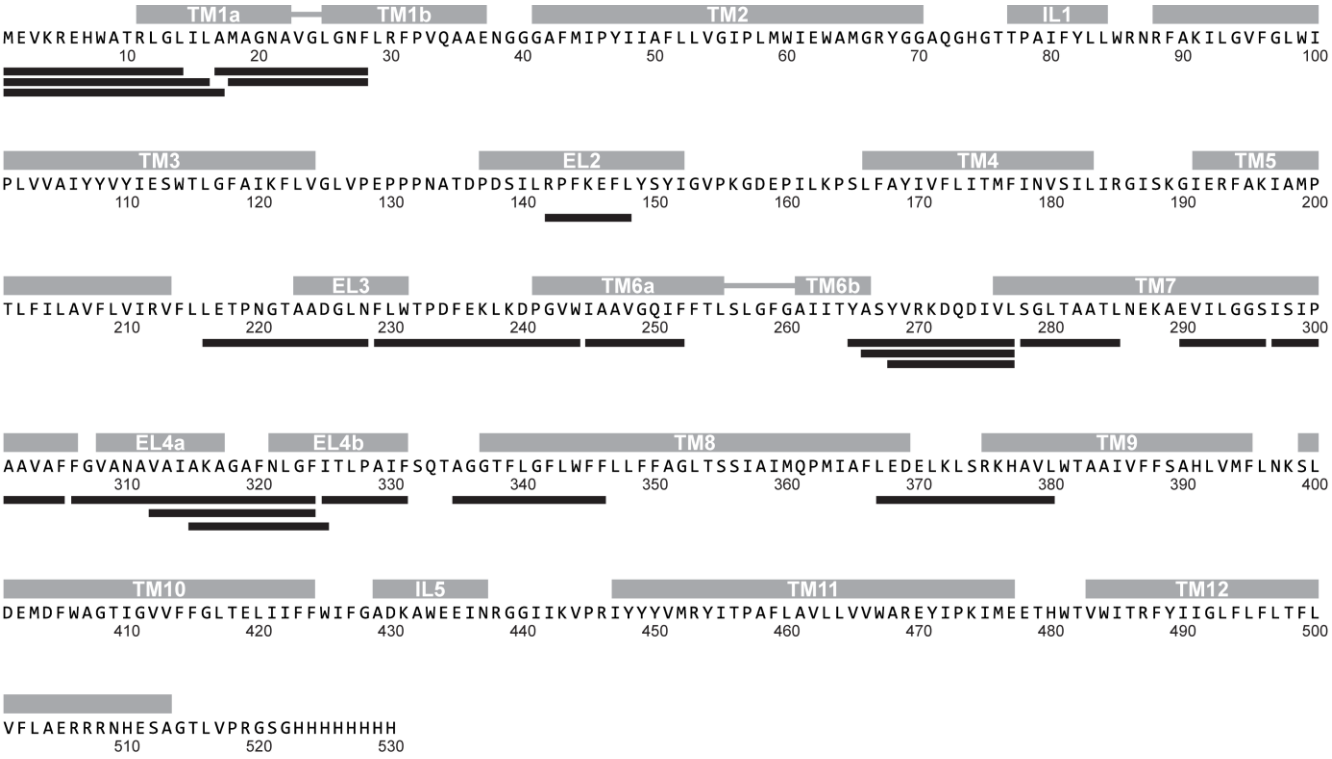

fig. S6. Sequence coverage map for LeuT reconstituted into phospholipid-containing bilayer nanodiscs. Offline pepsin proteolysis yielded a total of 21 peptides suitable for local HDX-MS analysis. The identified peptides are depicted as black bars and are aligned with the corresponding LeuT sequence. The peptides cover 30% of the protein sequence. Individual structural motifs in LeuT are indicated above the protein sequence in grey color. Notably, due to the increased sample complexity for nanodisc-embedded LeuT, we could not achieve the same high sequence coverage as for detergent-solubilized LeuT (cf. Fig. 1A).

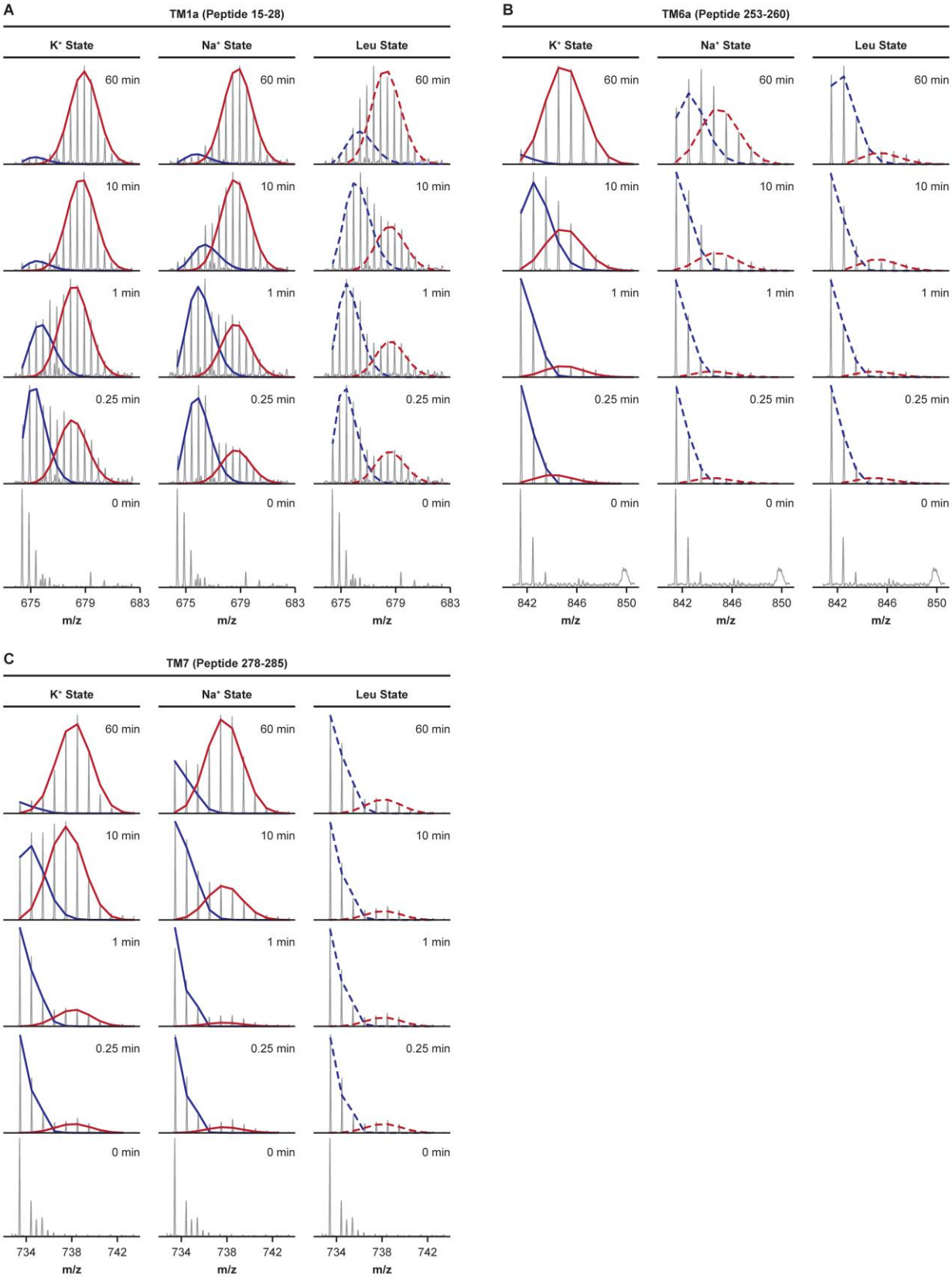
A
TM1a (Peptide 15-28)
K+ State
Na+ State
Leu State
60 min
10 min
1 min
0.25 min
0 min
675
679
683
m/z
B
TM6a (Peptide 253-260)
842
846
850
C
TM7 (Peptide 278-285)
734
738
742

fig. S7. Na^+- and substrate-induced stabilization of TM helices. Representative mass spectra for individual peptides covering (**A**) TM 1a (peptide 15-28), (**B**) the substrate binding site in TM 6 (peptide 253-260), and (**C**) the intracellular half of TM 7 (peptide 278-285) are shown for the K^+, Na^+, and Leu state and all sampled time-points. The bimodal isotopic envelopes can be fitted to a low- (blue) and high-mass (red) population. Bimodal deconvolution was accomplished using HX Express 2.0 (solid lines). In some instances, bimodal deconvolution did not result in a qualitatively meaningful fit and the depicted low- and high-mass population (dashed lines) was adjusted manually for visual guidance. Notably, for all peptides shown above, addition of Na^+ or the combination of Na^+ and leucine substantially decreased the rate of correlated exchange relative to the K^+ state.

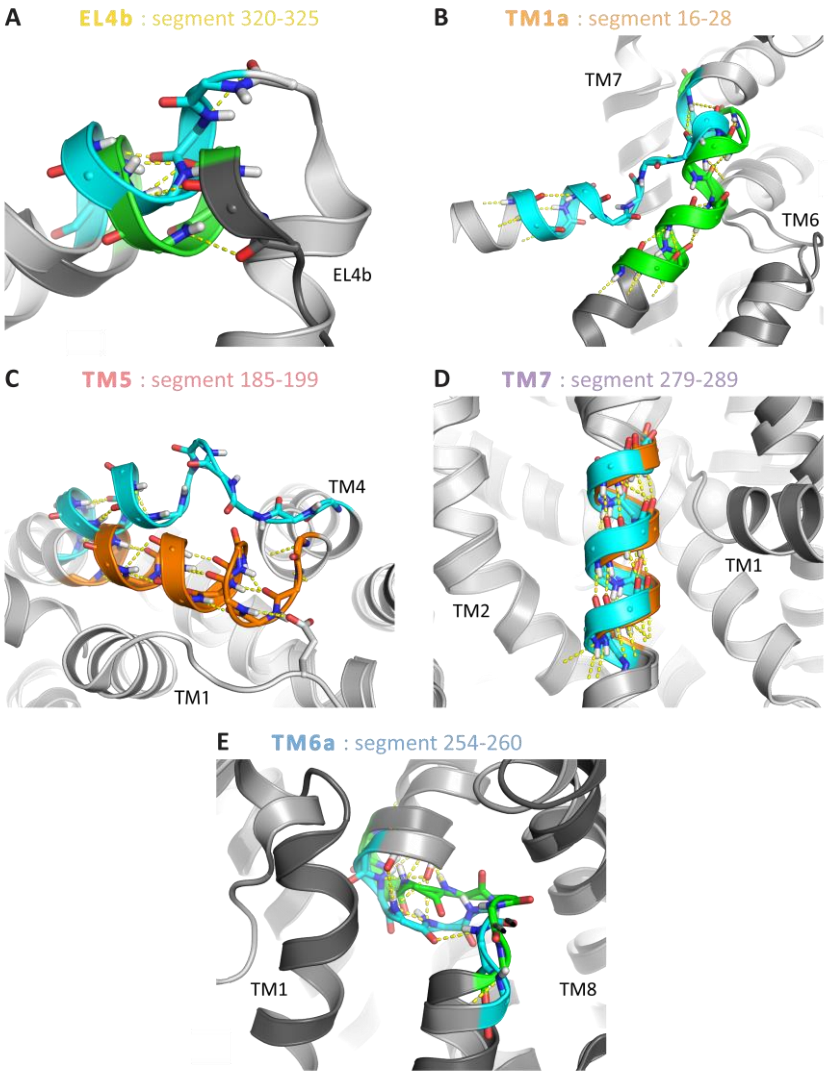

fig. S8. Compared conformations of EX1 segments in crystal structures. Each panel shows the two most different out of three selected X-ray structures: a ligand-bound, outward-occluded state (pdb 2A65, orange), an apo inward-open state (pdb 3TT3, cyan), and an apo outward-open return state (pdb 5JAE, green). Hydrogen bonds, defined with a donor-acceptor distance of 3.5 Å and an angle cutoff of 50°, are represented with dashed yellow lines. (**A**) EL4b segment 320-325 seen from the "inside", i.e. outwards from the approximate position of the ligand; (**B**) TM 1a segment 16-28 seen from the membrane plane. TM 5 and TM 8 have been removed for clarity; (**C**) TM 5 segment 185-199 seen from the intracellular side; (**D**) TM 7 segment 279-289 seen from the membrane plane; (**E**) TM 6a segment 254-260 seen from the membrane plane. TM 5 and TM 8 have been removed for clarity.

table S1. RMSD and hydrogen bond variations between three x-ray structures of LeuT for the EX1 segments. For each segment, we indicate the number of deuteriums observed to be exchanged in the EX1 regime. The three selected X-ray structures represent a ligand-bound, outward-occluded state (pdb 2A65), an apo inward-open state (pdb 3TT3), and an apo outward-open return state (pdb 5JAE). We show the RMSD of backbone atoms of each EX1 segment between these X-ray structures after alignment on helical regions, which quantify some of the known large-scale rearrangements in the LeuT functional cycle (cf. fig. S8). For each segment, we also show the maximum variation in total number of hydrogen bonds (HBs) involving backbone amide groups between any two structures, as well as the maximum number of these hydrogen bonds that have changed between any two structures (i.e., the acceptor is different, or the hydrogen bond is formed/broken). All the details of the hydrogen bond analysis leading to these numbers can be found in table S2. The maximal variation numbers shown here indicate regions where crystallographic data accounts for large-scale conformational changes along the LeuT functional cycle that may be related to the EX1 regime HDX.

Location		**EL4b**	**TM1a**	**TM5**	**TM7**	**TM6a**
Segment		**320-325**	**16-28**	**185-199**	**279-289**	**254-260**
Number of deuteriums exchanged		4-5	9	7	8-9	4-5
RMSD [Å]	2A65 - 3TT3	2.7	6.6	5.8	1.2	1.8
	2A65 - 5JAE	1.1	1.7	0.4	0.4	1
	3TT3 - 5JAE	2.6	7.2	5.9	1	2.3
Max variation in HB number		1	4	8	0	0
Max number of different HBs		4	7	9	0	2

table S2. Detailed hydrogen bond analysis in three x-ray structures of LeuT for backbone amide groups in the EX1 segments. See table S2 for details on the structures. For each EX1 segment, the amide hydrogen bond donors are listed in the left-most column. The hydrogen-bonding partners detected with a donor-acceptor distance of 3.5 Å and an angle cutoff of 50° are listed in the following columns. For each peptide, the yellow cells indicate changes in the total number of hydrogen bonds, while green cells indicate the total number of amide group that changed its hydrogen-bonding partner between two structures. Numbers in the column labeled MAX represent the maximum absolute value variation, and are those reported in table S1.

	partner in 2a65	other	partner in 3tt3	other	partner in 5jae	other	changed btw 2a65 and 3tt3 ?	changed btw 2a65 and 5jae ?	changed btw 3tt3 and 5jae ?	MAX
EL4b										
PHE`320/N							FALSE	FALSE	FALSE	
ASN`321/N			ALA`319/O				TRUE	FALSE	TRUE	
LEU`322/N					GLY`318/O	ALA`319/O	FALSE	TRUE	TRUE	
GLY`323/N					PHE`320/O		FALSE	TRUE	TRUE	
PHE`324/N	PHE`320/O		ASN`321/O		PHE`320/O		TRUE	FALSE	TRUE	
ILE`325/N	ASN`321/O						TRUE	TRUE	FALSE	
count	**2**		**2**		**3**		**3**	**3**	**4**	**4**
Change wrt 2a65			**0**		**1**					
Change wrt 5jae	**-1**		**-1**							**1**
TM1a										
LEU`16/N	LEU`12/O		LEU`12/O		LEU`12/O		FALSE	FALSE	FALSE	
ALA`17/N	GLY`13/O	LEU`14/O	GLY`13/O		GLY`13/O		FALSE	FALSE	FALSE	
MET`18/N	LEU`14/O		LEU`14/O	ILE`15/O	LEU`14/O		FALSE	FALSE	FALSE	
ALA`19/N	ILE`15/O		ILE`15/O		ILE`15/O		FALSE	FALSE	FALSE	
GLY`20/N	LEU`16/O	ALA`17/O	LEU`16/O		LEU`16/O	ALA`17/O	FALSE	FALSE	FALSE	
ASN`21/N	ALA`17/O	MET`18/O			MET`18/O		TRUE	TRUE	TRUE	
ALA`22/N	MET`18/O				ALA`19/O		TRUE	TRUE	TRUE	
VAL`23/N	ALA`19/O	ASN`286/OD1					TRUE	TRUE	FALSE	
GLY`24/N	ASN`27/OD1		ASN`27/ND2		SER`355/OG		TRUE	TRUE	TRUE	
LEU`25/N	TYR`108/OH	LEU`601/O			ALA`22/O		TRUE	TRUE	TRUE	
GLY`26/N	LEU`601/O	LEU`519/OXT			GLY`24/O		TRUE	TRUE	TRUE	
ASN`27/N	GLY`24/O		GLY`24/O		VAL`23/O		FALSE	TRUE	TRUE	
PHE`28/N			GLY`24/O	LEU`25/O			TRUE	FALSE	TRUE	
count	**12**		**8**		**11**		**7**	**7**	**7**	**7**
Change wrt 2a65			**-4**		**-1**					
Change wrt 5jae	**1**		**-3**							**4**
TM5										
ARG`185/N	ILE`182/O				ILE`182/O		TRUE	FALSE	TRUE	
GLY`186/N	LEU`183/O				LEU`183/O		TRUE	FALSE	TRUE	
ILE`187/N	GLU`6/OE2	GLU`6/OE1			GLU`6/OE2		TRUE	FALSE	TRUE	
SER`188/N	GLU`6/OE1						TRUE	TRUE	FALSE	
LYS`189/N							FALSE	FALSE	FALSE	
GLY`190/N	GLY`186/O				GLY`186/O		TRUE	FALSE	TRUE	
ILE`191/N	GLY`186/O				GLY`186/O		TRUE	FALSE	TRUE	
GLU`192/N	ILE`187/O				ILE`187/O		TRUE	FALSE	TRUE	
ARG`193/N	SER`188/O				SER`188/O		TRUE	FALSE	TRUE	
PHE`194/N	GLY`190/O		ILE`191/O		GLY`190/O		TRUE	FALSE	TRUE	
ALA`195/N	ILE`191/O		ILE`191/O		ILE`191/O		FALSE	FALSE	FALSE	
LYS`196/N	GLU`192/O	ARG`193/O	GLU`192/O		GLU`192/O	ARG`193/O	FALSE	FALSE	FALSE	
ILE`197/N	PHE`194/O		PHE`194/O		ARG`193/O	PHE`194/O	FALSE	TRUE	TRUE	
ALA`198/N	PHE`194/O		PHE`194/O		PHE`194/O		FALSE	FALSE	FALSE	
MET`199/N	ALA`195/O		ALA`195/O		ALA`195/O		FALSE	FALSE	FALSE	
count	**14**		**6**		**13**		**9**	**2**	**9**	**9**
Change wrt 2a65			**-8**		**-1**					
Change wrt 5jae	**1**		**-7**							**8**
TM7										
GLY`279/N	ILE`275/O		ILE`275/O		ILE`275/O		FALSE	FALSE	FALSE	
LEU`280/N	VAL`276/O		VAL`276/O	TRP`60/NE1	VAL`276/O		FALSE	FALSE	FALSE	
THR`281/N	LEU`277/O	SER`278/O	LEU`277/O		LEU`277/O		FALSE	FALSE	FALSE	
ALA`282/N	SER`278/O		SER`278/O		SER`278/O		FALSE	FALSE	FALSE	
ALA`283/N	GLY`279/O		GLY`279/O		GLY`279/O		FALSE	FALSE	FALSE	
THR`284/N	LEU`280/O		LEU`280/O		LEU`280/O	THR`281/O	FALSE	FALSE	FALSE	
LEU`285/N	THR`281/O		THR`281/O		THR`281/O		FALSE	FALSE	FALSE	
ASN`286/N	ALA`282/O	LA`283/O	ALA`282/O		ALA`282/O		FALSE	FALSE	FALSE	
GLU`287/N	ALA`283/O		ALA`283/O		ALA`283/O		FALSE	FALSE	FALSE	
LYS`288/N	THR`284/O	LEU`285/O	THR`284/O		THR`284/O		FALSE	FALSE	FALSE	
ALA`289/N	LEU`285/O		LEU`285/O	A/ASN`286/O	LEU`285/O		FALSE	FALSE	FALSE	
count	**11**		**11**		**11**		**0**	**0**	**0**	**0**
Change wrt 2a65			**0**		**0**					
Change wrt 5jae	**0**		**0**							**0**
TM6a										
THR`254/N	GLN`250/O		GLN`250/O		GLN`250/O	ILE`251/O	FALSE	FALSE	FALSE	
LEU`255/N	ILE`251/O	PHE`252/O	ILE`251/O	PHE`252/O	ILE`251/O		FALSE	FALSE	FALSE	
SER`256/N	PHE`252/O	PHE`253/O	PHE`252/O	PHE`253/O	PHE`252/O		FALSE	FALSE	FALSE	
LEU`257/N	PHE`252/O		PHE`252/O		PHE`252/O		FALSE	FALSE	FALSE	
GLY`258/N	GLU`62/OE2				GLU`62/OE2		TRUE	FALSE	TRUE	
PHE`259/N			SER`256/O				TRUE	FALSE	TRUE	
count	**5**		**5**		**5**		**2**	**0**	**2**	**2**
Change wrt 2a65			**0**		**0**					
Change wrt 5jae	**0**		**0**							**0**